Calculation of the friction, diffusion and sedimentation coefficients of nanoplatelets of arbitrary shape

José G. Hernández-Cifre*, Ricardo Rodríguez-Schmidt,
Carmen M. Almagro-Gómez, José García de la Torre
Departamento de Química Física, Facultad de Química,
Campus de Excelencia Regional *Mare Nostrum*,
Universidad de Murcia, 30100 Murcia, Spain

October 24, 2022

Abstract

We have developed a computational scheme for the calculation of the hydrodynamic properties of nanoplatelets – or flat sheets – of arbitrary shape based on the bead-modelling methodology. The procedure has been implemented in computer codes that interface with the public-domain `HYDRO++` program. When the friction coefficient calculated for the model is normalised to the value of an infinitely thin disk having the same surface area, its dependence on thickness normalised to a characteristic length of the platelet surface is very weak and depends just on the shape of the particle and not on its size. This allows for a simplified, general treatment of the dependence on thickness. In addition to examples with various peculiar shapes, we have calculated the friction coefficient of elliptical particles as well as some regular polygons. The results are presented in the form of simple equations relating the friction coefficient to the particle dimensions. The results for the friction coefficient are applied to the formulation of the experimentally measurable diffusion and sedimentation coefficients. The diffusion coefficient has a very weak dependence on thickness so that it can be employed to analyse the geometry of the surface even if the thickness is not precisely determined. However, the sedimentation coefficient depends appreciably on thickness and can be used for its precise determination. A joint analysis of diffusion and sedimentation can provide a complete determination of the nanoplatelet shape, dimensions and mass.

1 Introduction

Since the seminal work of A. Einstein, it is well known that the size of particles can be estimated from measurements of simple properties in dilute solution or suspension, like diffusion coefficients and viscosities [1]. Shortly after his work, T. Svedberg invented the technique of analytical ultracentrifugation (AUC), having as a main purpose the determination of size distribution of colloidal gold particles [2]. When applied to proteins (for instance, serum albumin [3]), it was found that they sedimented not as polydisperse aggregates of amino acids, but as single, well defined species. This finding was essential to establish the macromolecular concept.

Since those early works, the properties of biomacromolecules and synthetic polymers in solution are regarded as essential sources of information on their conformation (size, shape, flexibility, etc) [4–6]. The relationship between such structural aspects and the measured properties for flexible or rigid, rod-like chains was initially done in terms of bead models, consisting of strings of frictional elements – the beads – connected by spring-like or fixed-length connectors [7, 8]. The solution dynamics of the bead models is described in terms of the hydrodynamic interaction (HI) effect.

In the realm of biological macromolecules, the very specific structures adopted by proteins, nucleic acids and macromolecular complexes presented the challenge of modelling in detail their peculiar shapes. For many years, rigid biomacromolecules, like globular proteins, were simply modelled as revolution ellipsoids [9]. The possibility of using bead models for representing such peculiar shapes was put forward by Bloomfield and coworkers [10, 11]. Their rationale was that a rigid particle of arbitrary shape could be modelled as a cluster of identical or unequal spherical beads, with HI effects treated in a manner inspired in the above mentioned treatments for polymer chains. The complexity of such treatment for arbitrarily shaped bead models would not allow an analytical treatment, but computer procedures could be designed for that purpose.

Nowadays, the bead modelling methodology is well developed and implemented in computer programs that allow the calculation of solution properties like the hydrodynamic coefficients of diffusion and sedimentation, the intrinsic viscosity, and even more complex features, like nuclear magnetic resonance relaxation. Thus, the `HYDRO++` program is devised for user-constructed bead models of arbitrary shape [12], and `HYDROSUB` is for beads-shell models of cylindrical and ellipsoidal subunits [13]. Particularly useful are `HYDROPRO` and `HYDRONMR` that build the model directly from a list of atomic coordinates contained in a PDB file [14–16].

Hydrodynamic properties of nanoparticles in suspension, like diffusion coefficients which are readily determined from dynamic light scattering (DLS) [17–20] and sedimentation coefficients obtained by analytical ultracentrifugation (AUC) [21–24], are particularly useful for the determination of the size and shape of the nanoparticles. Furthermore, various modern optical and electrochemical techniques, like optical trapping [25] and nanoimpact chronoamperometry [26], also provide values of diffusion coefficients.

Many nanoparticles adopt spherical shapes whose hydrodynamic coefficients are trivially evaluated from the classical Einstein equation. But there are also quite interesting non-spherical nanoparticles and some workers have already used bead-model based procedures to relate their shapes to measured hydrodynamic properties. Such is the case for short nanorods whose dimensions have been determined from translational and rotational diffusion coefficients obtained from dynamic light scattering (DLS), which were interpreted [27,28] using the numerical data for bead-shell models of cylinders [29]. Other illustrative examples are the analysis of DLS data of oligomeric clusters of gold nanoparticles arranged in well defined geometric (triangular, tetrahedral, etc) shapes [30–32], and the modelling of hybrid gold-DNA nanoparticles, in which a few gold nanospheres are joined by rigid DNA oligonucleotide linkers, that were characterized by analytical ultracentrifugation [33].

Bead-modelling tools have been conceived having in mind three-dimensional shapes. Corpuscular particles are somehow predominant in the fields of structural biology and colloid science. However, two-dimensional objects, i.e. flat, thin platelets or sheets can also be found in both fields. Some natural clays produce colloidal suspensions of platelets [34]. Platelets can be readily obtained from some metal hydroxides, with gibbsite (aluminum hydroxide) being a typical example. Graphite can also be prepared as flat sheets [35]. Similar particles can be envisioned and obtained with new nanotechnologies; for instance, engineered flat particles (nanoplatelets) can be made with biological materials, with the DNA origami being a relevant example [36], and even one-atom-thin sheets of graphene are available [37, 38]. Recent preparative methods with a variety of materials (gold or silver, oxides and sulphides, peptides, etc) allow the production of nanoplatelets of precisely controlled shapes like equilateral, triangular and hexagonal shapes [39–43]. In other instances, the platelets present arbitrary, irregular shapes which can be precisely characterized by electron microscopy.

For flat, thin nanoplatelet particles, the only theoretical results available, which have been employed by some authors to analyse the hydrodynamic properties, have been the infinitely thin disk [26, 44–47], which overlooks effects arising by the small thickness, and oblate revolution ellipsoids [48–51], which present the unrealistic feature of having a variable thickness which is maximum at its center and zero at the border. And, evidently, the circular surface is not appropriate for structures either regular, like triangular ones, or those with complex or irregular shapes.

The purpose of this work has been the development of a theoretical framework and computational procedures to be used for the prediction of properties of thin nanoplatelets of arbitrary shape. The scheme is an adaptation of the bead-modelling methodology to flat, thin structures. The procedure yields results for the friction coefficient from which the experimentally observable diffusion and sedimentation coefficients can be obtained.

2 Background and scope

The procedures presented in this paper are based in the bead-modelling methodology which is widely employed for the calculation of solution properties of colloidal particles and macromolecules with a rigid shape which is represented by a rigid array of N spherical elements with radii σ_i, with $i = 1, ...N$, that reproduces the size and shape of the particle. The theory and computer implementation of bead-modelling has been described in previous publications [12, 52]. Nonetheless, we present here a summary of the concepts and theory on which the program used in the present procedure, `HYDRO++`, is based.

The main starting data is just a list of the coordinates of the beads, $\mathbf{r}_i = (x_i, y_i, z_i)$, and their radii σ_i. The hydrodynamic properties are calculated from the frictional forces experienced by the beads, taking into account the hydrodynamic interaction (HI) that the motion of one bead affects the force experienced by the other ones. The HI effect is described by the HI interaction tensor, a symmetric 3×3 matrix for each pair of elements (i, j) given by

$$\mathbf{T}_{ij} = (8\pi\eta_0 R_{ij})^{-1}\left(\mathbf{I} + \frac{\mathbf{R}_{ij}\mathbf{R}_{ij}}{R_{ij}^2} + \frac{\sigma_i^2 + \sigma_j^2}{R_{ij}^2}\left(\frac{1}{3}\mathbf{I} - \frac{\mathbf{R}_{ij}\mathbf{R}_{ij}}{R_{ij}^2}\right)\right), \tag{1}$$

where $\mathbf{R}_{ij} = \mathbf{r}_j - \mathbf{r}_i$ is the distance vector between that pair of elements and η_0 is the solvent viscosity. Then, a $3N \times 3N$ "diffusion supermatrix" $\mathcal{B}$ is constructed with the 3×3 blocks $\mathbf{B}_{ij} = \mathbf{T}_{ij}$ if $i \neq j$, and $\mathbf{B}_{ii} = (1/\zeta_i)\mathbf{I}$, where $\zeta_i = 6\pi\eta_0\sigma_i$ is the Stokes' law friction coefficient of i-th bead and $\mathbf{I}$ is the 3×3 identity matrix. Eq. (1) was derived for non-overlapping beads of different sizes [11]. In our models, beads are identical and tangent but not overlapping with radii σ, and Eq. (1) reduces to the Rotne-Prager-Yamakawa tensor [53, 54], which is profusely employed in polymer hydrodynamics.

Then, a $3N \times 3N$ "friction supermatrix" is calculated as the inverse of the diffusion supermatrix, $\mathcal{C} = \mathcal{B}^{-1}$, and from $\mathcal{C}$, three 3×3 friction tensors, $\mathbf{\Xi}_{tt}$, $\mathbf{\Xi}_{rr}$, $\mathbf{\Xi}_{tr}$, corresponding to translation, rotation and translation-rotation coupling, can be calculated [52]. These tensors are the blocks of the 6×6 friction tensor of the particle, which is inverted to obtain the 6×6 diffusion tensor of the particle, according to a generalized Einstein relationship:

$$\mathcal{D} = \begin{pmatrix} \mathbf{D}_{tt} & \mathbf{D}_{tr}^T \\ \mathbf{D}_{tr} & \mathbf{D}_{rr} \end{pmatrix} = k_B T \begin{pmatrix} \mathbf{\Xi}_{tt} & \mathbf{\Xi}_{tr}^T \\ \mathbf{\Xi}_{tr} & \mathbf{\Xi}_{rr} \end{pmatrix}^{-1}. \tag{2}$$

The superscript T indicates transposition. If the origin of the chosen system of coordinates is not the particle's center (which will be the case for irregular particles), a transformation of the $\mathbf{D}_{tt}$ tensor is required to be referred to the so-called center of diffusion [52]. Finally, from the $\mathbf{D}_{tt}$ and $\mathbf{D}_{rr}$, the hydrodynamic coefficients which characterize the translational and rotational dynamics of the rigid particle can be evaluated. Thus, the overall translational diffusion coefficient, measurable from dynamic light scattering and other techniques, is obtained as

$$D = (1/3)Tr(\mathbf{D}_{tt}) = (D_{tt}^{xx} + D_{tt}^{yy} + D_{tt}^{zz})/3, \tag{3}$$

and the friction coefficient is simply evaluated from the conventional Einstein relationship, $f = k_B t/D$, where k_B is the Boltzmann constant and T is the absolute temperature.

The treatment of rotational diffusion is more complex. The properties related to rotation (e.g. depolarized dynamic light scattering, electric birefringence decay, etc) depend on up to five relaxation times, $\tau_k, k = 1, ...5$, which are derived from the eigenvalues of D_{rr}, and the dependencies are specific of each property. `HYDRO++` does report the values calculated for the full translational/rotational diffusion tensor, so that the numerical values of these quantities are available in any calculation. In the present paper, we have concentrated on properties related to translational diffusion, which are more experimentally accessible, with the main purpose of providing a general framework for hydrodynamic modelling of nanoplatelets and giving a viewpoint on how their hydrodynamic behavior depends on their structure(shape, size and thickness).

The bead-model methodology in `HYDRO++` calculates properties in the limit of infinite dilute solution. This is the usual condition for the experimental characterization of basic, overall features (mass, size, shape or conformation, etc) of macromolecules or nanoparticles. The concentration dependence of the solution or dispersion properties is, of course, of practical interest, but its interpretation requires a formalism quite different and more complex than the present one.

3 Method

Like all the methodologies in the `HYDRO` suite, the procedure proposed here for nanoplatelets is based on bead modelling, and is particularly inspired by the successful representation of the one-dimensional topology of filamentous particles as strings of touching beads. From the pioneering bead-modelling study of Kirkwood and coworkers [55, 56], it is known that a string of beads provides a proper hydrodynamic model of a cylindrical rod. Using a simplified treatment of hydrodynamic interactions (HI), these authors demonstrated that the bead model reproduces the results of the rod of length L and diameter d in the limit of very large aspect ratio $p = L/d$. A more detailed description of HI extended the agreement to finite p [57], and recently we have shown that, when evaluated by means of `HYDRO++`, a linear string of N touching beads of diameter b with length $L = Nb$ reproduces the results of cylindrical rods of length L if the bead diameter is chosen so that the volumes of the string of beads and that of the cylinder match, which holds when $b = \sqrt{3/2}d = 1.225d$ [58].

This situation for one-dimensional particles provides the rationale for the present procedure for bead-modelling planar, thin platelet nanoparticles, i.e. nanoplatelets. They will be represented as planar arrays of touching beads with spacing equal to their diameter, b, and radius $\sigma = b/2$, arranged, for simplicity, in an hexagonal, closest-packing lattice. The contour of the nanoplatelet is superimposed onto that planar network of beads with spacing b. Some criterion is devised to specify whether or not a node in the network belongs to the particle, i.e. lies within the contour. The bead diameter, b, should be related to the thickness, h, in such a way that the volume of the bead model would equalize that of the platelet given by Ah, where A is the platelet surface area.

The implementation of our procedure requires an algorithm to place the beads. First, maximum and minimum values are specified for the coordinates of the points belonging to the nanoplatelet surface so that the contour is fully included within a rectangle with lower-left and upper-right corners (x_{min}, y_{min}) and (x_{max}, y_{max}), respectively. The rectangle is filled with a network of nodes. Finally, some criterion has to be specified to determine whether a node belongs to the nanoplatelet.

We have written two Fortran source codes that produce input files for the general program `HYDRO++` [12], following the scheme of the `MultiHYDRO` code [59]. One of them, `HYDRO2D-Shape`, requires a section in the code in which the user has to program the condition fulfilled only by points within the nanoplatelet. As we shall describe later on, this can be done in a fairly simple way for any arbitrary shape which can be modelled as simple geometrical shapes like ellipses or polygons. The other code, named `HYDRO2D-Circles`, works with a specification of the nanoplatelet size and shape in terms of a set of touching or overlapping circles that closely reproduces the geometry of the nanoplatelet (indeed, it is a 2D analogue of the bead modelling with spherical elements in 3D).

For a surface area A, the number of nodes in an hexagonal lattice of spacing b, and therefore the number of touching beads, will be $N = (2/\sqrt{3})A/b^2 = 1.155A/b^2$. The volume equalization criterion requires that the volume of the N tangent beads of diameter b in the model is the same as that of the nanoplatelet, Ah. This condition leads to $h = 0.605b$, $b = 1.652h$ and $N = 0.423A/h^2$. The area A of the platelet surface is employed in the treatment of results, although it is not initially required for the hydrodynamic calculations. It can be trivially computed geometrically for simple models. For complex shapes, we can use the value calculated by the computer program for the number of beads, $A = (\sqrt{3}/2)Nb^2$.

Once the coordinates of the bead model of the nanoplatelet are determined, the calculation is done with the general bead-model program `HYDRO++`. It should be kept in mind that the `HYDRO++` calculation requires a computing time proportional to N^3. Nowadays, in an ordinary personal computer, computing time for $N = 3000$ is less than 10 seconds. Thus, calculations for nanoplatelets with a value of A/h^2 requiring up to nearly 3000 elements can be readily made. Very thin nanoplatelets, like monoatomic graphene platelets with even much larger A/h^2 would pose a computational problem but, as it will be shown below, such a problem can be conveniently solved.

The `HYDRO++` calculation reports the diffusion and sedimentation coefficients, D and s, which are in turn obtained from the translational friction coefficient, f [4–6]. As described below, the evaluation of these coefficients requires values for the temperature and several quantities pertaining to the solvent and solute. However, the hydrodynamic behaviour is primarily determined by the size and shape of the particle whose influence can be jointly expressed by the equivalent radius:

$$a_T = \frac{f}{6\pi\eta_0}, \tag{4}$$

where η_0 is the solvent viscosity. The notation a_T follows the convention of denoting as a_X the radius of a sphere having a given value for property X [60], which in the present case is the translational friction coefficient. a_T is also commonly named Stokes radius (or simply hydrodynamics radius, R_h) as it is the value of a sphere which, according to the Stokes equation, would have the same frictional coefficient as the particle under consideration. We remark that a_T depends only on the geometry (size and shape) of the particle, and `HYDRO++` calculates this radius from just a list of Cartesian coordinates and radii of the beads in the bead model [29].

4 Results

4.1 Disks

The simplest case is that of a circular disk of radius R. Apart from its own interest as a model for some planar particles, it provides a most convenient check for our procedures because exact theoretical, analytical results, rigorously derived from fluid dynamics, are available for an infinitely thin disk [61–64].

For highly symmetric particles, like the disk and regular polygons, if the Cartesian system is centered at the particle's center, with the z axis perpendicular to the particles's plane, the translation-rotation tensor vanishes, $\mathbf{D}_{tr} = \mathbf{0}$ and $\mathbf{\Xi}_{tr} = \mathbf{0}$ in Eq. (2), and therefore the tt tensors follow an Einstein relationship $\mathbf{\Xi}_{tt} = (k_BT)^{-1}\mathbf{D}_{tt}$. Furthermore, the friction and diffusion tensors are diagonal, with the in-plane x and y axes, corresponding to motion perpendicular to the z axis, being identical and denoted by $\Xi_{tt}^{xx} = \Xi_{tt}^{yy} \equiv \Xi^{\perp}$, and the z component, corresponding to motion along the z axis, indicated as $\Xi_{tt}^{zz} \equiv \Xi^{\parallel}$. Thanks to this simplifications, the translational friction coefficient is given by:

$$\frac{1}{f} = \frac{1}{3}\left(\frac{2}{\Xi^{\perp}} + \frac{1}{\Xi^{\parallel}}\right). \tag{5}$$

The results from exact fluid-mechanic theory are $\Xi^{\perp} = (32/3)\eta_0 R$ and $\Xi^{\parallel} = 16\eta_0 R$.

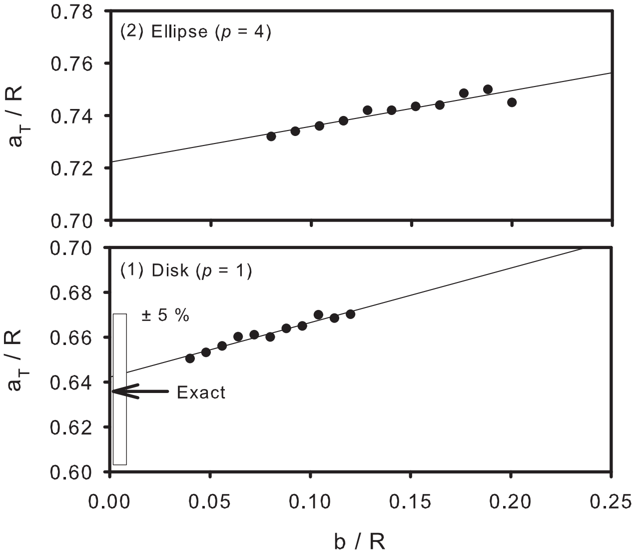

Figure 1: Plot of a_T vs. bead size b (equivalent thickness $h = 0.605b$), normalised to R. Results for (1) a disk ($p = 1$) of radius R, indicating a ±5% error bar over the exact result, and (2) an elliptical particle with large semiaxis $S = 4R$ ($p = S/R = 4$).

Placing these values in Eq. (5), we find

$$f = 12\eta_0 R, \tag{6}$$

and then, from Eq. (4), the hydrodynamic radius of an infinitely thin disk of radius R and area $A = \pi R^2$ is obtained:

$$a_{T;0} = \frac{2R}{\pi} = 0.6366R \quad \text{(infinitely thin disk)}, \tag{7}$$

where the additional subscript 0 indicates zero thickness.

We have carried out calculations for arrays of beads representing a disk with $R = 1$ in arbitrary units, and values of the lattice spacing (or bead diameter) b varying from 0.12 down to 0.04. The results show a linear dependence with the bead size or lattice spacing, b (platelet thickness is $h = 0.605b$, as indicated above), as displayed in Fig. 1. The extrapolation to zero thickness yields the result $a_{T;0} = 0.641R$, which is in excellent agreement (difference of less than 1%) with the exact theoretical value.

4.2 General treatment for arbitrarily shaped platelets

In order to express results in a systematic manner, we can first of all define a geometric radius equivalent to the area, A, i.e. the radius of a circle having the same area as the nanoplatelet, given by

$$a_A = (A/\pi)^{1/2} = 0.564A^{1/2}. \tag{8}$$

This value serves as a geometric reference to evaluate the thickness of the nanoplatelet, which will be expressed by the dimensionless ratio, h^*:

$$h^* = h/a_A = 1.772hA^{-1/2}. \tag{9}$$

Note that the reciprocal $1/h^*$ can be regarded as a general aspect ratio for any particle shape. For the treatment of hydrodynamic quantities, it can be useful to define other dimensionless ratios, like that of the friction coefficient of a nanoplatelet of arbitrary shape and thickness, f, referred to the value of the friction coefficient for a disk of the same area as the nanoplatelet and zero thickness given by

$$f_{A;0} = 12\eta_0 a_A, \tag{10}$$

so that

$$f/f_{A;0} = (\pi/2)(a_T/a_A) \tag{11}$$

or

$$f/f_{A;0} = (\pi^{3/2}/2)(a_T/A^{1/2}) = 2.785a_T A^{-1/2}. \tag{12}$$

The ratio $f/f_{A;0}$ will depend on the shape of the nanoplatelet and the dimensionless thickness h^*. The linear relationship that we have found for the thickness dependence in the results for disks suggests a general linear relationship:

$$f/f_{A;0} = C + Qh^*, \tag{13}$$

with

$$C \equiv (f/f_{A;0})(h^* = 0), \tag{14}$$

where the dimensionless constants C and Q will depend somehow on the shape of the nanoplatelet but not on its absolute size.

4.3 Results for arbitrarily shaped structures

With the procedure implemented in `HYDRO2D-Circles` and `HYDRO2D-Shape`, we have calculated f for a variety of structures. In addition to polygonal and elliptical particles, whose results are analysed in detail below, we have considered other constructs.

Using `HYDRO2D-Circles` we have modelled a "lollipop" shaped particle, with a disk attached to a stem, the latter being modelled as a string of tangent disks. Another "strange" structure is an arbitrary superposition of circles. Also, as another illustration of the code `HYDRO2D-Shape`, we have programmed a shape resulting of the intersection of two rectangles that resembles a "cross".

These structures are depicted in Fig. 2. In Fig. 3, it is confirmed that, like for circular particles, the dependence of $f/f_{A;0}$ is linear on h^*, as indicated in Eq. (13). Linear fits

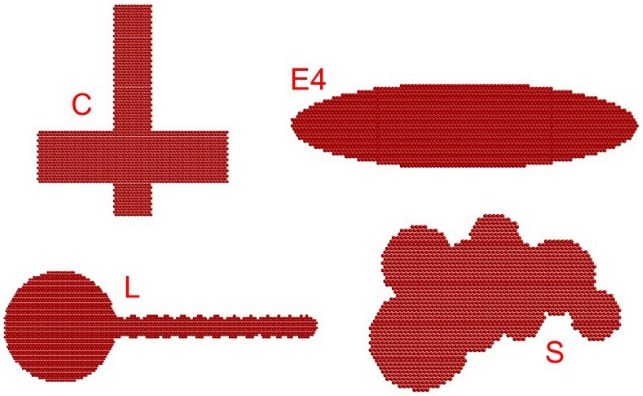

Figure 2: Examples of platelet shapes. The models depicted here have about $N \approx 2000$ beads (in calculations N reaches up to about 3000). The “cross” C and ellipses, here E4 with $p = 4$, were generated with `HYDRO2D-Shape`. The “lollipop” L and the “strange” S shapes were constructed with `HYDRO2D-Circles`.

provide the results listed in Table 1. The values of the slopes vary in the range 0.6 – 1.0, with an average $Q \approx 0.76$, but they are always quite small, so that the dependence on thickness, from the term Qh^*, is rather weak regardless of particle shape.

4.4 Elliptical and polygonal nanoplatelets

In the same way as the revolution, biaxial ellipsoid has been classically considered as the simplest model to reflect the deviation of a globular particle from the spherical shape, an elliptical shape can play the same role for planar particles. In order to study the dependence of the friction coefficient on the shape, we have carried out calculations for elliptical nanoplatelets with small and large semiaxes R and S (area $A = \pi RS$), varying the axial ratio $p = S/R$ (up to $p = 10$) and varying the thickness ratio, which for elliptical particles is $h^* = h/(RS)^{1/2}$ (see Eq. (9)). In all cases the linear relationship with thickness, Eq. (13), was verified, always finding that the slope is quite small. For some values of p, the thickness dependence and the extrapolation are shown in Fig. 3 and final results are collected in Table 1.

The dependence of the zero-thickness friction coefficient on p, when expressed in the form of $f/f_{A;0}$, is found to be linear for moderate values of p, as shown in Fig. 4. The interpolating equation $C \equiv (f/f_{A;0})(h^* = 0) = 1 + 0.0430(p - 1)$ reproduces the computed raw data with a precision of 1% or better. Furthermore, Q presents quite slight fluctuations around a value of about 0.85. Then, the following equation can describe the frictional coefficient of elliptical particles (for $p < 10$):

$$f/f_{A;0} = 1 + 0.0430(p - 1) + 0.85h^*. \tag{15}$$

Thus, the calculation of f from the dimensions of the elliptical platelets (R, S and h)

Table 1: Results for the parameters of the linear dependence expressed in Eq. (13) for several structures.

Code	Structure	C	Q
E1	Disk ($p = 1$)	1.005	0.79
E2	Ellipse ($p = 2$)	1.039	0.77
E4	Ellipse ($p = 4$)	1.136	0.81
E8	Ellipse ($p = 8$)	1.293	1.04
T	Equilateral Triangle	1.075	0.66
R1	Square ($p = 1$)	1.035	0.68
R2	Rectangle ($p = 2$)	1.035	0.68
R3	Rectangle ($p = 3$)	1.103	0.62
R6	Rectangle ($p = 6$)	1.213	0.65
H	Hexagon	1.011	0.78
S	"Strange"	1.076	0.82
L	"Lollipop"	1.267	0.88
C	"Cross"	1.195	0.71

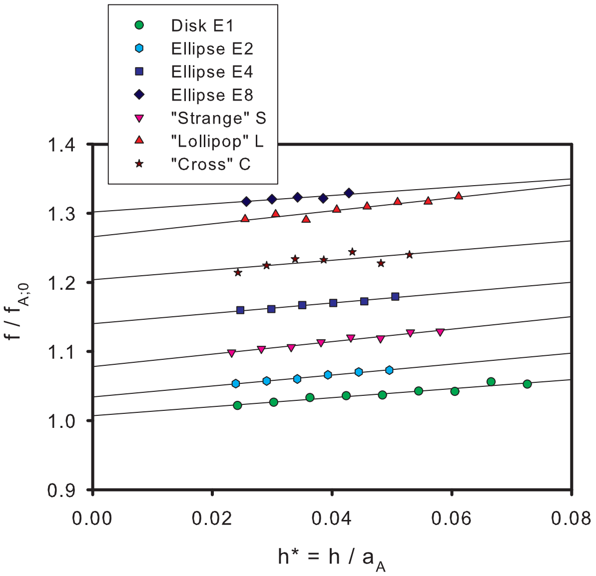

Figure 3: Plot of the reduced frictional coefficient, $f/f_{A;0}$, vs. the reduced thickness, h^*, for the platelet shapes shown in Fig. 2 and some other elliptical shapes (E1 or Disk, E2 and E8).

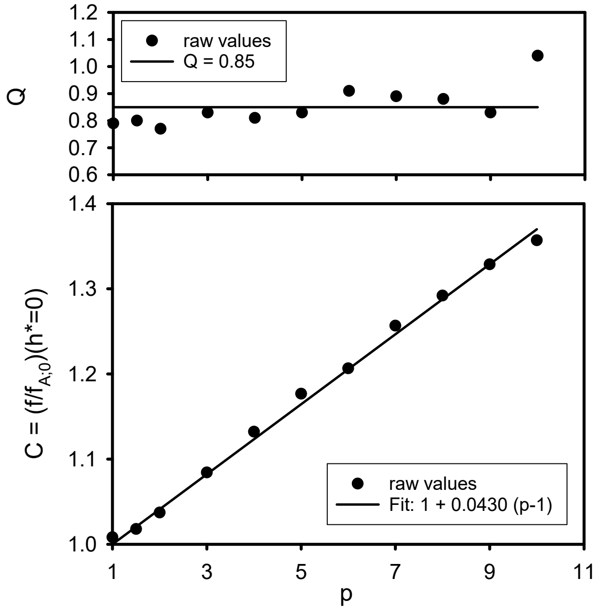

Figure 4: Dependence of the constants in Eq. (13) for elliptical particles on the axial ratio, p.

can be straightforwardly carried out since $p = R/S$, $f_{A;0} = 12\eta_0(RS)^{1/2}$ (from Eqs. (8) and (10)), and $h^* = h(RS)^{-1/2}$ (from Eq. (9)).

As mentioned in the Introduction, carefully controlled preparation methods yield nearly perfect regular polygonal shapes, mainly triangular and hexagonal. Results for these shapes are included in Table 1. It is noteworthy that for hexagonal platelets the shape-dependent ratio $f/f_{A;0}$ is nearly unity – the value for the disk –, while for the triangular platelet is 6% greater. Values for square and rectangular shapes with various aspect ratios (namely $p = 3$ and $p = 6$) are also listed in Table 1.

5 Treatment of experimental data: diffusion and sedimentation

In the preceding section, we formulated results in the form of a frictional ratio $f/f_{A;0}$ that depends only on the shape parameters, C and Q, and the reduced thickness, h^*, in order to present a simple, general form (Eq. (13)) for the dependence on size (A and h) and shape. Explicit equations for the friction coefficient and the hydrodynamic radius are:

$$f = 12\eta_0(\pi^{-1/2}A^{1/2}C + Qh) \tag{16}$$

and

$$a_T = 2(\pi^{-3/2}A^{1/2}C + Q\pi^{-1}h) = 0.359A^{1/2}C + 0.637Qh. \tag{17}$$

We remark that the dependency of f and a_T on the thickness h is linear. In the calculation for an arbitrary particle as described above, the bead model would be constructed using either `HYDRO2D-Circles` or `HYDRO2D-Shape`, and the subsequent run of `HYDRO++` provides the results for f and a_T. If the thickness h of the nanoplatelet is so small that the number of beads N in the model is too high, one would run calculations for a series of larger h values which would require lower N values, and a final result for the particle's h could be obtained by linear extrapolation.

The determination of structural features of macromolecular or colloidal particles from their frictional behaviour is mainly carried out by measurements of the diffusion coefficient, D, and the sedimentation coefficient, s. D is related to the friction coefficient, f, by the Einstein equation

$$D = k_B T / f, \tag{18}$$

where k_B is the Boltzmann constant and T is the absolute temperature.

As mentioned in the Introduction, the most frequently used technique for measuring D is dynamic light scattering [17–20]. Nowadays, simple benchtop instruments allow the determination of D and the hydrodynamic radius,

$$a_T = \frac{k_B T}{6\pi\eta_0 D}. \tag{19}$$

In the investigation of nanoplatelet structures using diffusion measurements by comparison of calculated and experimental results, the weak dependence of D and a_T on the thickness h gives the advantage that the results regarding the shape and dimensions of the surface would not be appreciably influenced by uncertainties in the thickness. But, conversely, diffusion data would not be appropriate for the determination of the nanoplatelet thickness.

Analytical ultracentrifugation is another powerful technique for hydrodynamic characterization [21–24]. Sedimentation velocity experiments provide the sedimentation coefficient of the particles, s, which is given by the ratio of the so-called buoyant mass of the particle, m_b, to the friction coefficient, f. When dealing with sedimentation of macromolecules in solution, we usually find in the literature the expression:

$$s = \frac{M(1 - \bar{v}\rho_s)}{N_A f}, \tag{20}$$

where M is the molecular mass of the solute and N_A is the Avogadro's number, so that M/N_A is the mass m of the solute particles. The buoyant mass is $m_b = m(1 - \bar{v}\rho_s)$, where $\bar{v}$ and ρ_s are the specific volume of the solute and the density of the solution (nearly equal to the solvent density for a dilute solution).

We consider that an equivalent but more appropriate formalism when dealing with nanoparticles would employ the particle's mass, m, and the densities for the particles – which is that of the material they are made of –, ρ_p, and that of the suspension, ρ_s, which again may be taken as that of the solvent at the high dilutions used in sedimentation velocity experiments. Then, the buoyant mass is $m - m_s$, where the particle mass is $m = V\rho_p$, V being the particle volume, and $m_s = V\rho_s$ is the mass of a volume V of the suspension. Thus, the sedimentation coefficient is written as

$$s = \frac{m(1 - \rho_s/\rho_p)}{f}, \tag{21}$$

and using D in place of f we have

$$\frac{s}{D} = \frac{m(1 - \rho_s/\rho_p)}{k_B T}. \tag{22}$$

Eq. (22) is a particular form of the Svedberg's equation, which states that the ratio of sedimentation and diffusion coefficients gives the particle mass. Remarkably, this is valid for particles of any shape.

An explicit equation for the sedimentation coefficient of nanoplatelets can be written combining Eqs. (16) and (21):

$$s = \frac{(\rho_p - \rho_s)}{12\eta_0} \frac{Ah}{(\pi^{-1/2} C A^{1/2} + Qh)}. \tag{23}$$

In the treatment of diffusion and sedimentation coefficients of conventional 3D particles, a quantity that is frequently employed is the so-called frictional ratio, f/f_0, where f_0 is the friction coefficient of a spherical particle having the same volume as the particle under consideration. In sedimentation-velocity AUC, the computational procedures employed to analyse the time-dependent concentration profiles measured for the determination of s employ or report somehow this ratio. For a platelet whose volume is $V = Ah$, the radius of the sphere with such a volume is $a_V = (3V/4\pi)^{1/3}$, so that

$$f/f_0 = \frac{a_T}{a_V} = \left(\frac{4\pi}{3Ah}\right)^{1/3} a_T. \tag{24}$$

The hydrodynamic radius a_T could be either extracted from previous measurements of diffusion or evaluated with our computer programs.

In order to present numerical values illustrating the kind and strength of the dependence of both s and D on particle size, we show in Fig. 5 their variation with particle dimensions for triangular nanoplatelets, a shape frequently found among metallic nanoparticles [65–69] and other materials, like CdSe [70]. For this example, we employ results reported by Liebig et al. [71] for nearly monodisperse gold equilateral nanotriangles with a thickness $h = 7.5$ nm, edge length $L = 175$ nm, and area A = 1312 nm^2. We evaluate the hydrodynamic coefficients of such particles in water at 25^{o}C ($\rho_s = 0.997$ cm^3/g, $\eta_0 = 0.00891$ poise, and $\rho_p = 19.3$ cm^3/g for gold). Thus, D is evaluated from Eq. (18), where friction is given by Eq. (16), and s is evaluated from Eq. (23) using the values $C = 1.075$ and $Q = 0.66$ reported in Table 1 for equilateral triangles, obtaining $D = 5.11 \times 10^{-8}$ cm^2/s and $s = 2.26 \times 10^4$ S (in Svedberg units, 1 S = 10^{-13} s).

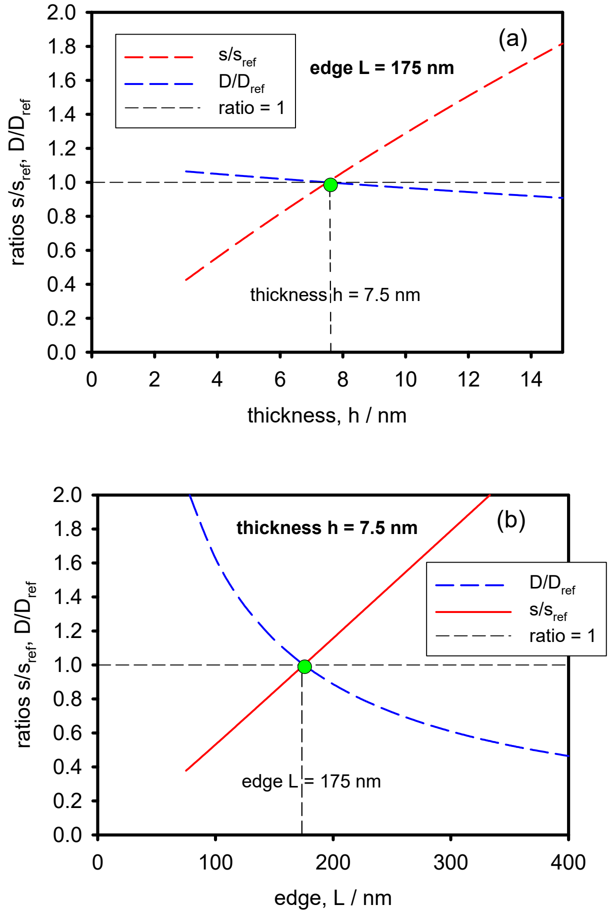

Figure 5: Ratios of the D and s of triangular platelets to those for a platelet with $L = 175$ nm and $h = 7.5$ nm. See text for more details.

Using these values as references (denoted D_{ref} and s_{ref}), we evaluate the effect of changing the dimensions L and h of the triangular platelet, calculating the ratio of s and D predicted for other dimensions to these reference values. The results are displayed in Fig. 5. Regarding the dependency on thickness h, Fig. 5(a) shows how D depends very weakly on h while s presents an appreciable and nearly linear dependency. Indeed, if the Qh term in Eq. (16) is neglected (such would be the case for a very thin platelet and a reasonable approximation in practical cases) then $f \propto A^{1/2} \propto L$. Thus, D does not depend (or depends very weakly) on the thickness, but depends inversely proportional to the edge length, $D \propto L^{-1}$, as observed in Fig. 5(b). For the sedimentation coefficient in that limit, Eq. (23) predicts $s \propto A^{1/2}h \propto Lh$, proportional to both L and h, as demonstrated by the nearly straight lines in Figs. 5(a) and 5(b).

In addition to the previous problem that combines diffusion and sedimentation coefficients, we present now some applications showing how the diffusion coefficient and the geometry of the nanoplatelet can be inferred from each other. Such is the case, studied by Kleshchanok et al. [48] of suspension of a clay, charge-stabilized gibbsite (aluminum hydroxide) nanoplatelets of hexagonal shape, and polydisperse in size, having a mean side length $\bar{L}$=44.2 nm (standard deviation 17%) and mean thickness $\bar{h}$ =7.7 nm (standard deviation 55%), in DMSO with viscosity $\eta_0 = 2 \times 10^{-3}$ mPa.s at 293 K. The authors first represented the nanoplatelet as an infinitely thin circular disk, with radius $R = \bar{L}$ to obtain and estimation of the diffusion coefficient from Eq. 4.1, $D = 3.8 \times 10^{-12}$ m^2/s. When attempting to improve the estimate taking into account the appreciable thickness, considering a finite thick disk whose properties could be evaluated from the equations of Tirado and García de la Torre [60], they noticed that the aspect ratio, $p = \bar{h}/(2\bar{L})$=0.087 was below the limit $p > 0.1$ allowed by those equations, and opted to model the platelet as an oblate ellipsoid of revolution with the same p, obtaining $D = 3.1 \times 10^{-12}$ m^2/s. As commented above, the oblate ellipsoid is not an adequate model even for discoid particles because of its variable thickness.

We have carried out an estimation based on our procedures. For the structures whose values of C and Q have been evaluated here, a numerical calculation is easily done. The area A of the hexagonal platelet with side length $\bar{L}$=44.2 nm is $A = 5075$ nm^2. For the hexagon $C = 1.011$ and $Q = 0.78$ from Table 1. Then Eq. 16 gives the frictional coefficient f from which the diffusion coefficient is $D = 3.62 \times 10^{-12}$ m^2/s. From their DLS measurements, these authors obtained $D = 2.1 \times 10^{-12}$ m^2/s, somewhat smaller than those obtained from their own approximations. The experimental D value required extrapolation to zero angle and zero concentration, and their effects, and possibly the effect of polydispersity, could be the reasons for the deviation. Nonetheless, their approximation for the infinitely thin disk is close to our numerical result for the hexagon. The main reason is that the $C = 1.011$ value for the hexagon is very close to the value for the disk (theoretically $C = 1$), and the influences of non-circular shape and finite thickness may cancel each other.

Another experiment on nanoplatelet dynamics, now in the field of electrochemistry, is the study of nano-impact chronoamperometry, in which the diffusion-dependent occurrence of impacts of individual particles with a microelectrode is monitored. Compton and coworkers [26] have employed this technique in the characterization of graphene nanoplatelets for the determination of the potential of zero charge and their diffusion coefficient. Their graphene nanoplatelets have nearly square shape, with a width $L = 16.5 \pm 5$, area $A = 297 \pm 152$ μm and thickness 7.1 ± 2 nm, as determined from scanning electron microscopy. The ratio h/L (with $h^* = 0.00086$) is so small that the platelets can be regarded are infinitely thin. Having the infinitely thin disk as the only model available, the authors determined an estimated diffusion coefficient $D = 4 \times 10^{-14}$ m^2/s in aqueous solution. Following the same steps as for the hexagonal gibbsite, from the values of A, h and the coefficient $C = 1.035$ for square platelets (the term Qh in negligible for such small h) we obtain $D = 3.84 \times 10^{-14}$ again quite close to the value for the disk, as it happened with hexagonal platelets. However, the diffusion coefficient obtained from the analysis of the electrochemical experiment was $D = 2 \pm 0.8 \times 10^{-14}$ m^2/s which deviates appreciably from the theoretical calculations for both disks and squares. The authors first noted that the non-circular nature may cause deviations, but this is not the main cause. As noted in the final discussion of these authors, the reason is the wide polydispersity of the sample so that, as stated by the authors, “smaller area nanoplatelets are expected to have a higher diffusion coefficient... Therefore it is unsurprising that the experimentally estimated diffusion coefficient of the platelets is significantly faster than the calculated theoretical value, as faster diffusing platelets are more likely to impact the electrode than larger ones diffusing more slowly”. Remarkably this work reported a detailed characterization of the distributions of area and width, from which – hopefully – not a single, average value, but a distribution of diffusion coefficients could be predicted.

6 Conclusions

The bead-modelling methodology, which has been shown so useful for predicting the hydrodynamic properties of conventional 3D macromolecular and colloidal particles, has been adapted for the translational friction, diffusion and sedimentation coefficients of thin, planar nanoparticles. We have written simple computer programs that enable the calculation of those properties for nanoplatelets of arbitrary shape. Then, application is made to a variety of regular geometries like polygons or ellipses as well as other irregular shapes. When the friction coefficient and the particle thickness are conveniently normalised, simple relationships between them emerge.

We remark that the combination of diffusion and sedimentation coefficients can provide a full characterization of the platelet’s geometry. The diffusion coefficient depends essentially on the size and shape of the platelet surface, but it is quite insensitive to its thickness h. On the other hand, the sedimentation coefficient is roughly proportional to h (as it follows from Eq. (23) if the small term Qh is neglected), so that knowing the area A and the shape coefficient C, h can be estimated. Even more directly, from Eq. (22) the ratio s/D provides the particle’s mass $m = \rho_p V$ from which its volume would be $V = m/\rho_p = Ah$ and $h = m/(\rho_p A)$.

A primary purpose in experimental studies of characterization of nanoplatelets regards the shape and lateral dimensions of their surface. Recent advances have allowed the control of the platelet thickness h and demonstrated its important influence in a variety of relevant properties [72, 73]. Our work shows that the measurement of hydrodynamic coefficients of nanoplatelets in suspension can be quite useful for a full characterization of their shape and size. From other point of view, our study of the influence of size and shape of the nanoparticles in hydrodynamic coefficients can be useful to analyse the experimental data in order to elucidate other aspects of the particles’ suspension that may be influencing their behaviour. The work reported in this paper is a proof-of-concept that provides procedures for hydrodynamic modelling of nanoparticles and an overview of their hydrodynamics that we intend to extend to other properties like rotational diffusion and solution viscosity. Also, it is our intention to adapt the procedure to further aspects like polydispersity.

Funding

Support was provided by grant CTQ2017-85425-P from MICINN (Spain) and grant 20933/PI/18 from Fundación Séneca (Comunidad Autónoma de la Región de Murcia).

CRediT authorship contribution statement

José G. Hernández-Cifre: Validation, Investigation, Data Curation, Writing - Review & Editing. **Ricardo Rodríguez-Schmidt:** Programming, Investigation. **Carmen M. Almagro-Gómez:** Visualization, Investigation. **Jose García de la Torre**: Conceptualization, Methodology, Data Curation, Writing - Original Draft, Supervision, Project administration, Funding acquisition.

Declaration of Competing Interest

The authors declare that they have no known competing financial interests or personal relationships that could have appeared to influence the work reported in this paper.

Data availability: computer programs

`HYDRO2D-Circles` and `HYDRO2D-Shape` are simple Fortran90 codes that produce data files for a `HYDRO++` calculation. They and their codes will be freely available, along with documentation and examples, in our Web site:
http://leonardo.inf.um.es/macromol.

Acknowledgements

This article is dedicated to the memory of Prof. Javier Martínez Salazar with whom we maintained a friendly and fruitful communication.

References

[1] A. Einstein, A new determination of molecular dimensions, Ann. Physik 19 (1906) 289–306. (English translation in: "Investigation on the Theory of the Brownian Movement", Dover, New York, 1956).

[2] T. Svedberg, H. Rinde, The ultra-centrifuge, a new instrument for the determination of size and distribution of sizes of particles in macroscopic colloids, J. Am. Chem. Soc. 46 (1924) 2677–2693.

[3] T. Svedberg, B. Sjögren, The molecular weights of serum albumin and of serum globulin, J. Am. Chem. Soc. 59 (1928) 3318–3332.

[4] K.E. van Holde, W. Johnson, P. Ho, Principles of Physical Biochemistry, 2nd Edition, Prentice Hall, Upper Saddle River, N.J., 1998.

[5] M. Rubinstein, R.H. Colby, Polymer Physics, Oxford University Press, Oxford, 2003.

[6] P.C. Hiemenz, T.P. Lodge, Polymer Chemistry, 2nd Edition, CRC Press, Boca Raton, 2007.

[7] J.G. Kirkwood, J. Riseman, The intrinsic viscosities and diffusion constants of flexible macromolecules in solution, J. Chem. Phys. 16 (1948) 565–573.

[8] B.H. Zimm, Dynamics of polymer molecules in dilute solution. Viscoelasticity, flow birefringence and dielectric dispersion, J. Chem. Phys. 24 (1956) 269–278.

[9] C. Tanford, Physical Chemistry of Macromolecules, J. Wiley and Sons, New York, 1961.

[10] V.A. Bloomfield, W.O. Dalton, K.E. Van Holde, Frictional coefficients of multisubunit structures. I. Theory, Biopolymers 5 (1967) 135–148.

[11] J. García de la Torre, V.A. Bloomfield, Hydrodynamic properties of macromolecular complexes. I. Translation, Biopolymers 16 (1977) 1747–1763.

[12] J. García de la Torre, G. Del Río Echenique, A. Ortega, Improved calculation of rotational diffusion and intrinsic viscosity of bead models for macromolecules and nanoparticles, J. Phys. Chem. B 111 (2007) 955–961.

[13] J. García de la Torre, B. Carrasco, Hydrodynamic properties of rigid macromolecules composed of ellipsoidal and cylindrical subunits, Biopolymers 63 (2002) 163–167.

[14] J. García de la Torre, M.L. Huertas, B. Carrasco, Calculation of hydrodynamic properties of globular proteins from their atomic-level structures, Biophys. J. 78 (2000) 719–730.

[15] J. García de la Torre, M.L. Huertas, B. Carrasco, HYDRONMR: Prediction of NMR relaxation of globular proteins from atomic-level structures and hydrodynamic calculations, J. Magn. Reson. 147 (2000) 138–146.

[16] D. Amorós, A. Ortega, J. García de la Torre, Prediction of hydrodynamic and other solution properties of rigid proteins from atomic- and residue-level models, Biophys. J. 101 (2011) 892–898.

[17] R. Pecora, Dynamic light scattering measurement of nanometer particles in liquids, J. Nanopart. Res. 2 (2000) 123–131.

[18] H. Hans, X. Liu, L. Austin, G. Maes, Q. Huo, Dynamic light scattering as a powerful tool for gold nanoparticle bioconjugation and biomolecular binding sites, Anal. Chem. 81 (2009) 9425–9432.

[19] C. Geers, L. Rodríguez-Lorenzo, D. Andreas Urban, C. Kinnear, A. Petri-Fink, S. Balog, A new angle on dynamic depolarized light scattering: number-averaged size distribution of nanoparticles in focus, Nanoscale 8 (2016) 15813–15821.

[20] P.M. Carvalho, M.R. Felicio, N.C. Santos, S. Gonsalves, M.M. Domingues, Application of light scattering techniques to nanoparticle characterization and development, Front. Chem. 6 (2018) 237.

[21] H. Cölfen, Analytical ultracentrifugation of nanoparticles, In H.S. Nalwa, editor, Encyclopedia of Nanoscience and Nanotechnology, volume 1, pages 67–88, American Scientific Publishers, Los Angeles, 2004.

[22] W. Mächtle, L. Börger, Analytical ultracentrifugation of polymers and nanoparticles, Springer, Berlin, 2006.

[23] V. Mittal, A. Völkel, H. Cölfen, Analytical ultracentrifugation of model nanoparticles: comparison of different analysis methods, Macromol. Biosci. 10 (2010) 754–762.

[24] K.L. Planken, H. Cölfen, Analytical ultracentrifugation of colloids, Nanoscale 2 (2010) 1849–1869.

[25] C. Pin, B. Cluzel, C. Renault, D. Peyrade, E. Picard, E. Hadju, F. de Fornet, Optofluid taming of a colloidal dimer with a silicon nanocavity, Appl. Phys. Lett. 108 (2014) 171108.

[26] J. Poon, C. Batchelor-McAuley, K. Tschulik, R.G. Compton, Single graphene nanoplatelets: capacitance, potential of zero charge and diffusion coefficient, Chem. Sci. 6 (2015) 2869–2876.

[27] R. Nixon-Luke, G. Bryant, A depolarized dynamic light scattering method to calculate translational and rotational diffusion coefficients of nanorods. Part. Part. Syst. Char. 36 (2019) 1800388.

[28] J. Rodríguez-Fernández, J. Pérez-Juste, L.M. Liz-Marzán, P.R. Lang, Dynamic light scattering of short Au rods with low aspect ratio, J. Phys. Chem. C 11 (2007) 5020–5025.

[29] A. Ortega, J. García de la Torre, Hydrodynamic properties of rodlike and disklike particles in dilute solution, J. Chem. Phys. 119 (2003) 9914–9919.

[30] M. Hoffmann, C.S. Wagner, L. Hernau, A. Wittemann, 3D Brownian diffusion of submicron sized particle clusters. ACS Nano 3 (2009) 3326–3334.

[31] R. Stuckert, C.S. Plüish, A. Wittemann, Experimental assessment and model validation on how shape determines sedimentation and diffusion of colloidal particles, Langmuir 34 (2018) 13339–13351.

[32] G.L. Hunter, K.V. Edmon, M.T. Elsesser, E.R. Weeks, Traking rotational diffusion of colloidal clusters, Opt. Express 19 (2011) 17189–17202.

[33] M.J. Urban, I.T. Holder, M. Schmid, V. Fernández Espín, J. García de la Torre, J.S. Hartig, H. Cölfen, Shape analysis of DNA-Au hybrid particles by analytical ultracentrifugation, ACS Nano 10 (2016) 7418–7427.

[34] F. Bergaya, B.K.G. Theng, G. Lagaly, editors, Handbook of clay science, Elsevier, Amsterdam, 2006.

[35] D.D.L. Chung, Exfoliation of graphite, J. Materials Sci. 22 (1987) 4190–4198.

[36] C.E. Castro, F. Kilchherr, D. Kim, E.L. Shiao, T. Wauer, P. Wortmann, M. Bathe, H. Dietz, A primer to scaffolded DNA origami, Nature Meth. 8 (2011) 221–229.

[37] M. Jacoby, Graphene: carbon as thin as can be, Chem. Eng. News 87 (2009) 14–20.

[38] M. Terrones, Controlling the shapes and assemblages of graphene, Proc. Natl. Acad. Sci. U.S.A. 109 (2012) 7951–7952.

[39] H. Cölfen, S. Yu, Y. Mastai, Formation and optical properties of gold nanoparticles synthesized in presence of double-hydrophilic block copolymers, J. NanoSci. Nanotech. 4 (2004) 291–298.

[40] W. Lu, Y. Ding, Y. Chen, Z.L. Wang, J. Fang, Bismuth telluride hexagonal nanoplatelets and their two-step epitaxial growth, J. Am. Chem. Soc. 127 (2005) 10112–10116.

[41] L. Leon, W. Su, H. Matsui, R. Tu, Interfacial templating of inorganic nanostructures using a growth directing and reducing peptide, Soft Matter 7 (2011) 10285–10290.

[42] S. Viabitskaya, A. Teulle, A. Cuche, J. Sharma, G. Girard, E. Dujardin, A. Arbouet, Morphology-induced redistribution of surface plasmon modes in two-dimensional crystalline gold platelets, Appl. Phys. Lett. 103 (2013) 131112.

[43] Q. Zeng, Q. Li, W. Li, X. Bin, J. Song, Higly sensitive homegenous immunoassays based on construction of silver triangular nanoplates-quantum dots FRET system, Sci. Rep. 6 (2016) 26534.

[44] Y.S. Cheng, H.C. Yehand, M.D. Allen, Dynamic shape factor of a plate-like particle, Aerosol Sci. Tech. 8 (1988) 109–123.

[45] F.M. van der Kooij, A.P. Philipse, J.K.G. Dhont, Sedimentation and diffusion in suspension of sterically stabilized colloidal platelets, Langmuir 16 (2000) 5317–5323.

[46] X. Yang, C. Guo, L. Ji, Y. Tu, Liquid crystalline and shear-induced properties of aqueous solution of graphene oxide sheets, Langmuir 29 (2013) 8103–8107.

[47] A.M. Philippe, C. Baravian, V. Bezughy, J.R. Angilella, F. Meneau, J. Bihannic, L.J. Michot, Rheological study of two-dimensional very anisometric colloidal particle suspensions: from shear-induced orientation to viscous dissipation. Langmuir 29 (2013) 5315–5324.

[48] D. Kleshchanok, M. Heinen, G. Nägele, P. Holmqvist, Dynamics of charged gibbsite platelets in the isotropic phase. Soft Matter 8 (2012) 1584–1592.

[49] M. Zimbone, E. Messina, G. Compagnini, M.E. Fragalà, L. Calcagno, Resonant depolarized dynamic light scattering of silver nanoplatelets, J. Nanopart. Res. 17 (2015) 402.

[50] P. Arenas-Guerrero, G.R. Iglesias, A.V. Delgado, M.L. Jiménez, Electric birefringence spectroscopy of montmorillonite particles, Soft Matter 12 (2016) 4923–4931.

[51] S.S. Bhandari, K. Muralidhar, Y.M. Joshi, Thermal diffusivity and viscosity of suspensions of disk-shaped nanoparticles, Ind. Eng. Chem. Res. 52 (2013) 15114–15123.

[52] B. Carrasco, J. García de la Torre, Hydrodynamic properties of rigid particles. Comparison of different modelling and computational procedures, Biophys. J. 76 (1999) 719–730.

[53] J. Rotne, S. Prager, Variational treatment of hydrodynamic interaction on polymers, J. Chem. Phys. 50 (1969), 4831-4837.

[54] H. Yamakawa, Transport properties of polymer chains in dilute solutions. Hydrodynamic interaction, Chem. Phys. 53 (1970), 436-443.

[55] J. Riseman, J.G. Kirkwood, The intrinsic viscosity, translational and rotatory diffusion constants of rod-like macromolecules in solution. *J. Chem. Phys.*, 18 (1950) 512–516.

[56] J.G. Kirkwood, P.L. Auer, The visco-elastic properties of solutions of rod-like macromolecules, J. Chem. Phys. 19 (1951) 281–287.

[57] H. Yamakawa, G. Tanaka. Translational diffusion coefficients of rodlike polymers: Application of the modified Oseen tensor, J. Chem. Phys. 57 (1972) 1537–1546.

[58] D. Amorós, A. Ortega, J. García de la Torre, Hydrodynamic properties of wormlike macromolecules: Monte Carlo simulation and global analysis of experimental data, Macromolecules 44 (2011) 5788–5797.

[59] J. García de la Torre, A. Ortega, H.E. Pérez Sánchez, J.G. Hernández Cifre, MULTIHYDRO and MONTEHYDRO: Conformational search and Monte Carlo calculation of solution properties of rigid and flexible macromolecular models, Biophys. Chem. 116 (2005) 121–128.

[60] A. Ortega, J. García de la Torre, Equivalent radii and ratios of radii from solution properties as indicators of macromolecular conformation, shape, and flexibility, Biomacromolecules 8 (2007) 2464–2475.

[61] A. Oberbeck, Ueber stationäre flüssigkeitsbewegungen mit berücksichtigung der inneren reibung, J. Reine Angew. Math. 81 (1876) 62–80.

[62] H. Lamb, Hydrodynamics, 6th Edition, p. 605, Dover, New York, 1945.

[63] G.K. Batchelor, An Introduction to Fluid Mechanics, Cambridge University Press, Cambridge, England, 1967.

[64] J. Happel, H. Brenner, Low Reynolds Number Hydrodynamics, p. 180, Noordhoff, Leiden, 1973.

[65] L. Scarabelli, M. Coronado-Puchau, J.J. Giner-Casares, J. Langer, L.M. Liz-Marzán, Monodisperse gold nanotriangles: size control, large-scale self-assembly, and performance in surface-enhanced Raman scattering, ACS Nano 8 (2014) 5833–5842.

[66] L. Scarabelli, L.M. Liz-Marzán, An extended protocol for the synthesis of monodisperse gold nanotriangles, ACS Nano 15 (2021) 18600–18607.

[67] F. Liebig, R.M. Sarhan, A. Reinecke, J. Koetz, "Green" gold nanotriangles: synthesis, purification by polyelectrolyte/micelle depletion flocculation and performance in surface-enhanced Raman scattering, RSC Adv. 6 (2016) 33561–33568.

[68] Y. Zhong, G. Liang, W. Jin, Z. Jian, Z. Wu, Q. Chen, Y. Cai, W. Zhang, Preparation of triangular silver nanoplatelets by silver seeds capped with citrate-CTA$^+$, RSC Adv. 8 (2018) 28934–28943.

[69] J.M. Kelly, G. Keegan, M.E. Brennan-Fournet, Triangular silver nanoparticles: their preparation, functionalization and properties, Acta Phys. Polonica 122 (2012) 337–345.

[70] N. Pinna, K. Weiss, H. Sack-Kongehl, W. Vogel, J. Urban, M.P. Pileni, Triangular CdS nanocrystals: synthesis, characterization and stability, Langmuir 17 (2001) 7982–7987.

[71] F. Liebig, R.M Sarhan, C.N.Z. Schmitt, A. Thrünemann, C. Prietzel, M. Bargheer, J. Koetz, Gold nanotriangles with crumble topping and their influence on catalysis and surface-enhanced Raman spectroscopy, ChemPlusChem 85 (2020) 519–526.

[72] S. Christodoulou, J.I. Clemente, J. Planelles, R. Brescia, M. Prato, B. Martín García, A. H. Khan, I. Moreels, Chloride-induced thickness control in CdSe nanoplatelets, Nano Lett. 18 (2018) 6248–6254.

[73] C. Otero-Martínez, J. Ye, J. Sung, I. Pastoriza-Santos, J. Pérez-Juste, A. Xia, A. Rao, R.L.Z. Hoye, L. Polavarapu, Colloidal metal-halide perovskite nanoplatelets: thickness-controlled synthesis, properties, and application in light-emitting diodes, Adv. Mater. 34 (2022) 2107105.

Highlights

- Development of methods for calculating hydrodynamic properties of nanoplatelets.
- Implementation in public-domain computer programs.
- Diffusion related to shape and surface dimensions but insensitive to thickness.
- Sedimentation and diffusion allow for whole characterization of the nanoplatelet.

José G. Hernández-Cifre: Validation, Investigation, Data Curation, Writing - Review & Editing. **Ricardo Rodríguez-Schmidt:** Programming, Investigation. **Carmen M. Almagro-Gómez:** Visualization, Investigation. **José García de la Torre:** Conceptualization, Methodology, Data Curation, Writing - Original Draft, Supervision, Project administration, Funding acquisition.

Declaration of interests

☒The authors declare that they have no known competing financial interests or personal relationships that could have appeared to influence the work reported in this paper.

☐The authors declare the following financial interests/personal relationships which may be considered as potential competing interests: